nature materials

LETTERS

PUBLISHED ONLINE: 28 FEBRUARY 2010 | DOI: 10.1038/NMAT2721

Template engineering of Co-doped $BaFe_2As_2$ single-crystal thin films

S. Lee[1], J. Jiang[2], Y. Zhang[3], C. W. Bark[1], J. D. Weiss[2], C. Tarantini[2], C. T. Nelson[3], H. W. Jang[1], C. M. Folkman[1], S. H. Baek[1], A. Polyanskii[2], D. Abraimov[2], A. Yamamoto[2], J. W. Park[1], X. Q. Pan[3], E. E. Hellstrom[2], D. C. Larbalestier[2] and C. B. Eom[1]*

Understanding new superconductors requires high-quality epitaxial thin films to explore intrinsic electromagnetic properties and evaluate device applications[1–9]. So far, superconducting properties of ferropnictide thin films seem compromised by imperfect epitaxial growth and poor connectivity of the superconducting phase[10–14]. Here we report new template engineering using single-crystal intermediate layers of (001) $SrTiO_3$ and $BaTiO_3$ grown on various perovskite substrates that enables genuine epitaxial films of Co-doped $BaFe_2As_2$ with a high transition temperature ($T_{c,\rho=0}$ of 21.5 K, where ρ = resistivity), a small transition width ($\Delta T_c = 1.3$ K), a superior critical current density J_c of 4.5 MA cm^{-2} (4.2 K) and strong *c*-axis flux pinning. Implementing $SrTiO_3$ or $BaTiO_3$ templates to match the alkaline-earth layer in the Ba-122 with the alkaline-earth/oxygen layer in the templates opens new avenues for epitaxial growth of ferropnictides on multifunctional single-crystal substrates. Beyond superconductors, it provides a framework for growing heteroepitaxial intermetallic compounds on various substrates by matching interfacial layers between templates and thin-film overlayers.

Epitaxial pnictide thin films have so far been hard to produce, especially the F-doped highest-T_c rare-earth 1111 phase[13,14]. As a result of both As and F being volatile at the deposition temperature, it is difficult to control the overall stoichiometry of the deposited film[13]. In contrast, Co, which can be used as the dopant in $Ba(Fe,Co)_2As_2$ (Ba-122), has a low vapour pressure under growth conditions. Alkaline-earth (AE) 122 phases have been grown on (001)-oriented $(La,Sr)(Al,Ta)O_3$ (LSAT) and $LaAlO_3$ (LAO) single-crystal substrates by us and other groups[10–12]. However, the quality of the films reported so far is not satisfactory because $T_{c,\rho=0}$ and ΔT_c are 14–17 K and 2–4 K, respectively, values that are much lower and broader than those of bulk single crystals[15]. Furthermore, J_c (5 K, self-field (SF)) of these films is ~10 kA cm^{-2}, one to two orders of magnitude lower than in bulk single crystals[15]. We believe a fundamental reason for the low quality of the AE-122 phase on these substrates is that AE-122 is a metallic system, which does not bond well with oxide single-crystal substrates. In particular, LSAT and LAO substrates contain trivalent cations, whereas the alkaline earths of Ba-122 or Sr-122 are divalent, making the bonding between the substrate and Ba-122 poor, which leads to a non-epitaxial, granular and poorly connected superconducting phase in which the grains are separated by high-angle grain boundaries, wetting grain-boundary phases such as FeAs and/or off-stoichiometric grains[16].

To overcome these problems, we explored the use of a template consisting of thin epitaxial layers of the divalent, AE-containing $SrTiO_3$ (STO) or $BaTiO_3$ (BTO) between various single-crystal perovskite substrates and the Ba-122 film. Building on this common feature, we propose the bonding model described in Fig. 1. Recently, we reported a proof-of-principle of this concept by growing Co-doped Ba-122 epitaxial thin films on (001)-oriented STO bicrystal substrates with intragrain J_c values over 1 MA cm^{-2} (4.2 K, SF), values significantly higher than in previously reported epitaxial thin films[17]. However, the STO substrates became electrically conducting during deposition of the Co-doped Ba-122 thin film at 730 °C in the high vacuum (2.7×10^{-5} Pa), owing to formation of oxygen vacancies in the STO (ref. 18). This provides a parallel, current-sharing path between Ba-122 and STO, which compromises normal-state property studies. Clearly, normal-state behaviour and potential device applications[19] need insulating substrates, especially microwave devices, which need substrates such as LSAT or LAO that have a low dielectric constant.

Here, we report single-crystal Co-doped Ba-122 epitaxial thin films using thin STO or BTO templates deposited on various perovskite single-crystal substrates, which include (001) LSAT, (001) LAO and (110) $GdScO_3$, all of which yield Ba-122 films with superior superconducting properties on insulating substrates. The 50–100 unit cell (u.c.)-thick STO and BTO templates were grown by pulsed laser deposition using a KrF excimer laser (248 nm) with high-oxygen-pressure reflection high-energy electron diffraction (RHEED) for digital control and *in situ* monitoring of the epitaxial growth[20]. Co-doped Ba-122 films ~350 nm thick were grown on both bare single-crystal substrates and substrates with STO and BTO templates. Structural and superconducting properties of these films are listed in Supplementary Table SI. We discuss here only films grown on bare STO, bare LSAT, STO/LSAT (that is, an STO template on LSAT) and BTO/LSAT, while emphasizing that similar properties were obtained on (001) LAO and (110) $GdScO_3$ too (see Supplementary Table SI).

Figure 2a and its inset show an atomic force microscope (AFM) image of a 100 u.c. STO template on LSAT and its RHEED pattern. They show atomically flat terraces and single-unit-cell-high (~4 Å) steps, which confirm that the STO template layer is as good as those of bulk single-crystal substrates of STO. It is found that an STO template up to 100 u.c. is fully coherent with the LSAT substrate. The epitaxial and crystalline quality of the Co-doped Ba-122 thin films was measured by four-circle X-ray diffraction

[1]Department of Materials Science and Engineering, University of Wisconsin-Madison, Madison, Wisconsin 53706, USA, [2]Applied Superconductivity Center, National High Magnetic Field Laboratory, Florida State University, 2031 East Paul Dirac Drive, Tallahassee, Florida 32310, USA, [3]Department of Materials Science and Engineering, The University of Michigan, Ann Arbor, Michigan 48109, USA. *e-mail: eom@engr.wisc.edu.

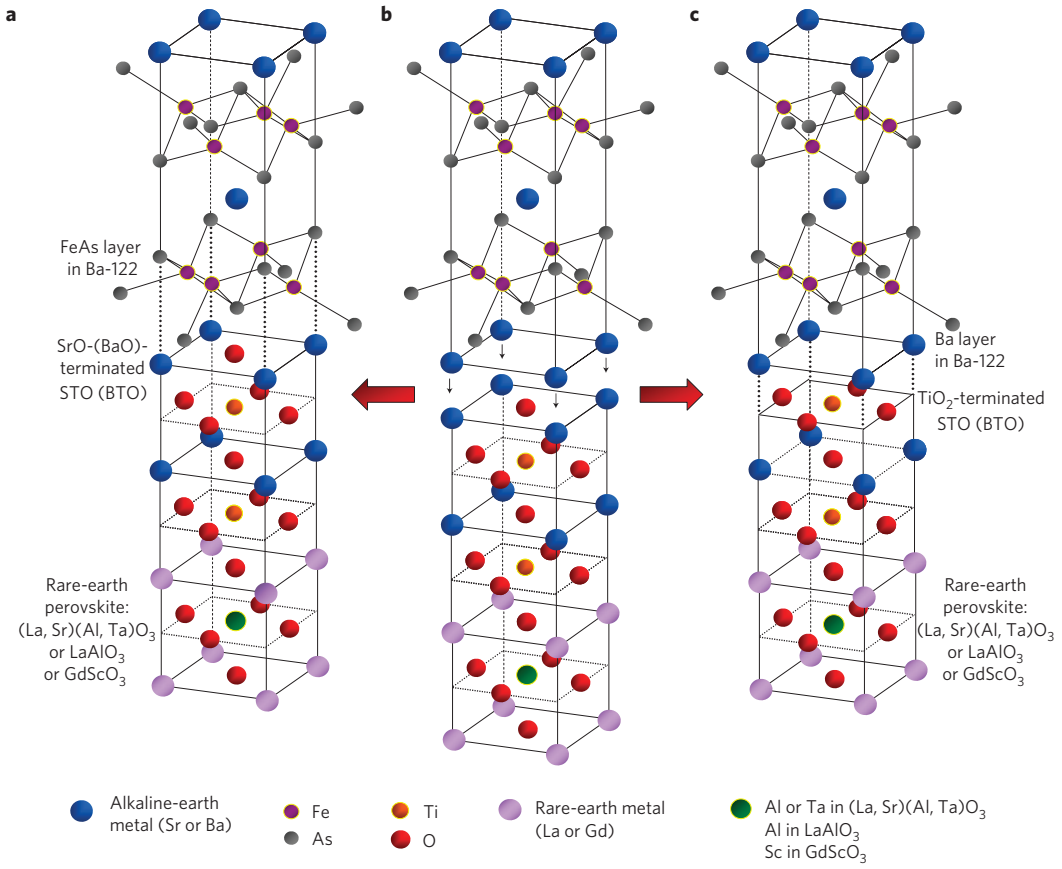

Figure 1 | Schematic model of Ba-122 deposition on a STO (BTO) template grown on various oxide substrates. a–c, The Ba-122 unit cell and the alkaline-earth titanium oxide (AETO) unit cells grown on a rare-earth (RE) perovskite oxide substrate unit cell (**b**). In this example, only two unit cells of AETO and one unit cell of RE perovskite are shown. There are two possible ways the Ba-122 and perovskite lattice bonding can occur. The FeAs layer in Ba-122 bonds strongly to RE-O-terminated RETO as Ba-122 is deposited (the AE-O layer from AETO replaces the Ba layer in Ba-122) (**a**). **c**, The Ba layer in Ba-122 bonds strongly to TiO_2-terminated RETO as Ba-122 is deposited (the Ba layer from Ba-122 replaces AE-O in the AETO) (**c**).

(XRD). Figure 2b shows the out-of-plane θ–2θ scans of the films on bare LSAT and 100 u.c. STO/LSAT. The XRD patterns show that the film 00l reflections dominate, which indicates c-axis growth normal to the template and substrate. An extra peak at $2\theta = \sim 65°$ in the film grown on STO/LSAT is the 002 reflection from Fe (ref. 11), however with an intensity of less than 0.5% of the Ba-122 (004) reflection. The intensity of the Ba-122 00l peaks on STO/LSAT is about two orders of magnitude higher than that on bare LSAT. This indicates that the film on STO/LSAT is highly c-axis oriented, whereas the film on bare LSAT is c-axis textured and polycrystalline. Rocking curves for the 004 reflection were measured to determine the out-of-plane mosaic spread and crystalline quality. As shown in Fig. 2c, the full-width at half-maximum (FWHM) of the 004 reflection rocking curve of the film on STO/LSAT is as narrow as 0.55°, which is the narrowest ever reported for AE-122 thin films, whereas that of the film on bare LSAT is as broad as 3.1°. Remarkably, the FWHM of the film on BTO/LSAT is as narrow as 0.17°, similar to that of a Ba-122 bulk single crystal[21] (see Supplementary Table SI).

In-plane texture and epitaxial quality were determined by azimuthal ϕ scans of the off-axis (112) peak, as shown in Fig. 2d. The film grown on bare LSAT shows broad major peaks ($\Delta\phi = 4.4°$) every 90° with extra broader intermediate-angle peaks, which indicates that the in-plane Ba-122 structure consists of grains with high-angle tilt grain boundaries. In contrast, the film grown on 100 u.c. STO/LSAT shows only sharp, strong peaks ($\Delta\phi = 0.8°$) every 90° characteristic of a truly epitaxial film with perfect in-plane texture. Our Ba-122 thin films are fully strain relaxed. The in-plane and out-of-plane lattice parameters of all of our Ba-122 films are the same as the bulk single-crystal values.

To verify the crystalline quality, microstructures were studied by transmission electron microscopy (TEM). Figure 3a–d shows the cross-sectional TEM images of the films grown on bare LSAT (Fig. 3a), 100 u.c. STO/LSAT (Fig. 3b), 20 u.c. STO/LSAT (Fig. 3c) and bare STO (Fig. 3d). The insets in the top right corners of Fig. 3a,b,d show the corresponding Ba-122 selected-area electron diffraction patterns, respectively. The Ba-122 films on bare STO and on STO-templated LSAT show epitaxial relationships between the films and the substrate, whereas the film on bare LSAT shows a granular microstructure with many misoriented grains. The inset on the left side of Fig. 3a shows the high-resolution TEM (HRTEM) image of a high-angle grain boundary in the Ba-122 film. The HRTEM image in Fig. 3c shows the structure of interfaces between STO and LSAT and between STO and Ba-122. The localized disorder of atomic arrangement at the STO/Ba-122 interface may be due either to interface reaction or to the ion beam damage during TEM sample preparation. The epitaxial films grown on bare STO and on STO/LSAT show vertically aligned line defects seen in the cross-sectional TEM images of Fig. 3b,d as well as in the top-left side inset in Fig. 3b. The inset in the bottom left corner of Fig. 3b shows a planar-view TEM image of the same film, revealing that the vertically aligned defects are uniformly distributed. Both X-ray energy dispersion spectroscopy and electron energy-loss spectroscopy reveal that the line defects consist of a secondary phase composed mainly of Ba and O and depleted of Fe, Co and As.

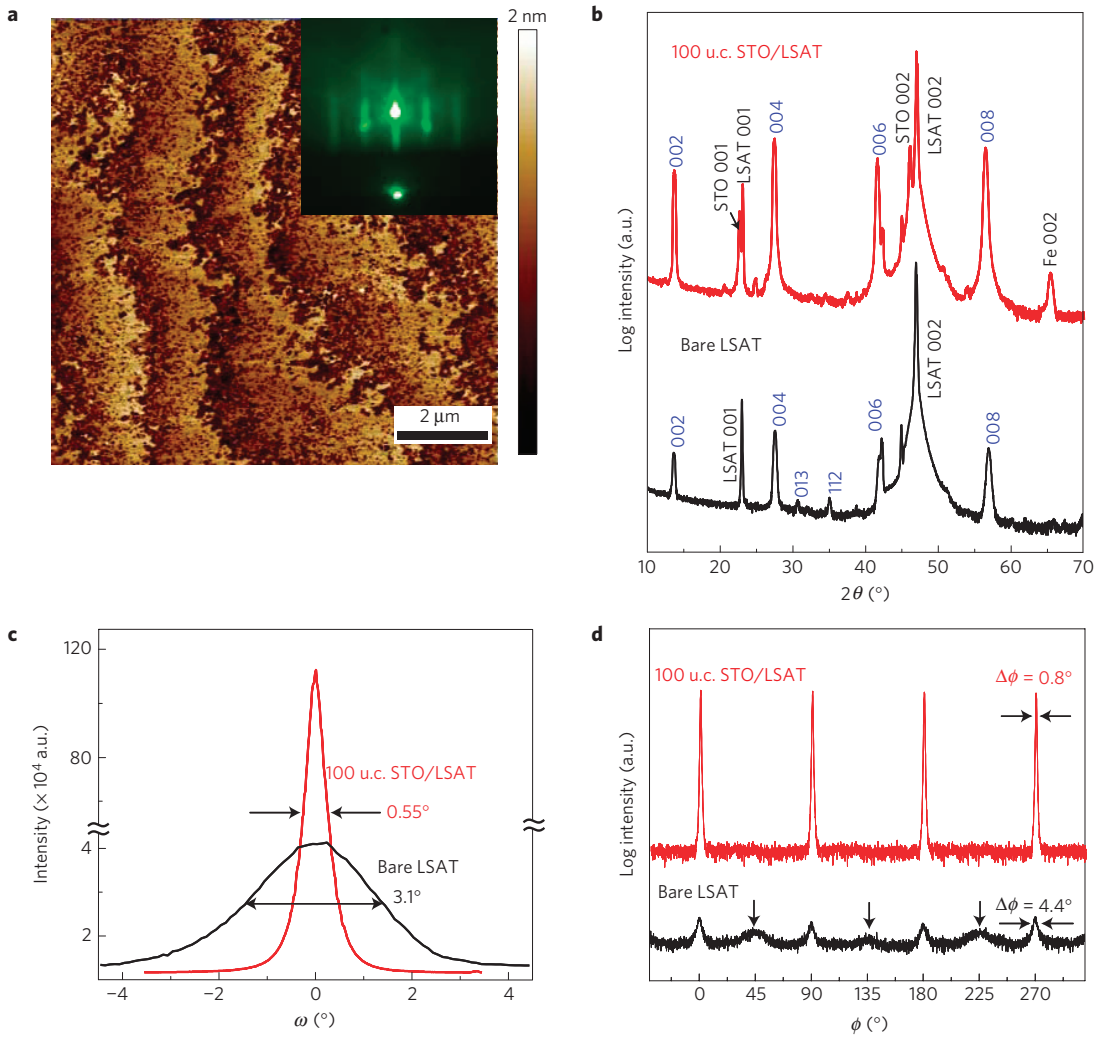

Figure 2 | AFM image and RHEED pattern of the STO template grown on LSAT, and XRD patterns obtained on the Co-doped $BaFe_2As_2$ thin films. **a**, AFM image of a 100 u.c. STO template grown on LSAT. The RHEED pattern of Ba-122 is shown in the inset. **b**, Out-of plane θ–2θ XRD patterns of the film grown on 100 u.c. STO/LSAT and the film grown on bare LSAT. All non-identified small peaks are reflections of identified peaks resulting from CuKβ and CuK$\alpha+\beta$. **c**, Rocking curve and FWHM for (004) reflection of Ba-122. **d**, Azimuthal ϕ scan and $\Delta\phi$ of the off-axis 112 reflection of Ba-122. The vertical arrows above the bare LSAT pattern indicate a peak resulting from misoriented grains separated by high-angle grain boundaries.

To characterize the superconducting transition temperature T_c, resistivity was measured as a function of temperature $\rho(T)$ by a four-point method. As shown in Fig. 4a, the residual resistivity ratio of the Ba-122 film grown on bare STO is as high as 160, a value consistent with oxygen-deficient STO (ref. 18) that we reproduced on bare STO substrates heated in vacuum under the same conditions used for Ba-122 deposition. In contrast, the residual resistivity ratios of films grown on STO/LSAT and BTO/LSAT templates were 1.8 and 2.4, respectively, values characteristic of Co-doped Ba-122 single crystals[22]. Furthermore, we noted that the room-temperature resistivity of a film on bare LSAT is much higher than a film grown on templated LSAT, which we interpret as being due to strong scattering at the high-angle grain boundaries. As shown in Fig. 4b, all films show high $T_{c,\rho=0}$ and narrow ΔT_c except for the film with high-angle grain boundaries grown on bare LSAT. In particular, $T_{c,\rho=0}$ of the film on 100 u.c. STO/LSAT is as high as 21.5 K and ΔT_c is as narrow as 1.3 K, which are the highest and narrowest values ever reported for AE-122 thin films.

Figure 4c shows the zero-field-cooled magnetization T_c transitions. All three epitaxial films have a strong diamagnetic signal, in contrast to the polycrystalline film grown on bare LSAT, which, as seen in the inset in Fig. 4c, shows a three orders of magnitude smaller diamagnetic signal than the epitaxial films. This is a clear indication of magnetic granularity associated with the inability of screening currents to develop across the high-angle grain boundaries in the film on bare LSAT.

Figure 5a shows J_c as a function of magnetic field for all films determined from vibrating sample magnetometer measurements in fields up to 14 T. Here too all films except that on bare LSAT show high J_c values, over 1 MA cm^{-2} (4.2 K, SF), which are the highest values ever reported for AE-122 thin films and are even better than in bulk single crystals (0.4 MA cm^{-2} at 4.2 K; ref. 15). Remarkably, the J_c of the film on BTO/LSAT is as high as ~4.5 MA cm^{-2}. Furthermore, the J_c values of the two epitaxial films on the templates have only a weak field dependence, indicative of little or no suppression of the J_c by strong fields, as indicated by the STO/LSAT film, which had J_c = ~0.4 MA cm^{-2} even at 14 T. The magneto-optical image of the film on STO/LSAT (inset in Fig. 5a) shows strong flux shielding and a J_c of ~3 MA cm^{-2} (6.6 K, 20 mT), similar to that deduced from the magnetization measurements. Such magneto-optical images confirm that the epitaxial films grown on STO/LSAT or BTO/LSAT are uniform and well connected without any weak links.

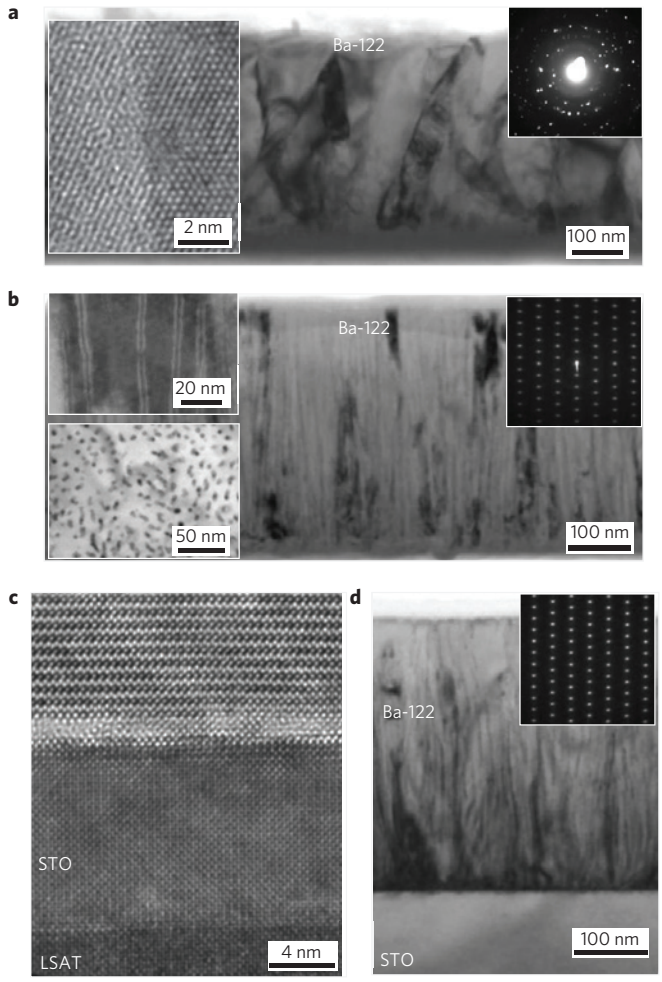

Figure 3 | Microstructures of Co-doped $BaFe_2As_2$ thin films investigated by TEM. a–d, Cross-sectional TEM micrographs of films on bare LSAT (**a**), 100 u.c. STO/LSAT (**b**), 20 u.c. STO/LSAT (**c**) and bare STO (**d**). They confirm that the films on bare STO or STO-buffered LSAT are epitaxial, whereas the film on bare LSAT is polycrystalline with misoriented grains. Line defects along the *c* axis exist in the films grown on STO/LSAT and bare STO. The insets on the left side of **b** are planar and cross-sectional views of the same film, showing a uniform distribution of the vertically aligned line defects. The insets on the top right sides of **a**,**b**,**d** show the corresponding selected-area electron diffraction patterns. The HRTEM image in **c** shows the interface structures between LSAT and 20 u.c. STO and between 20 u.c. STO and the Ba-122 film.

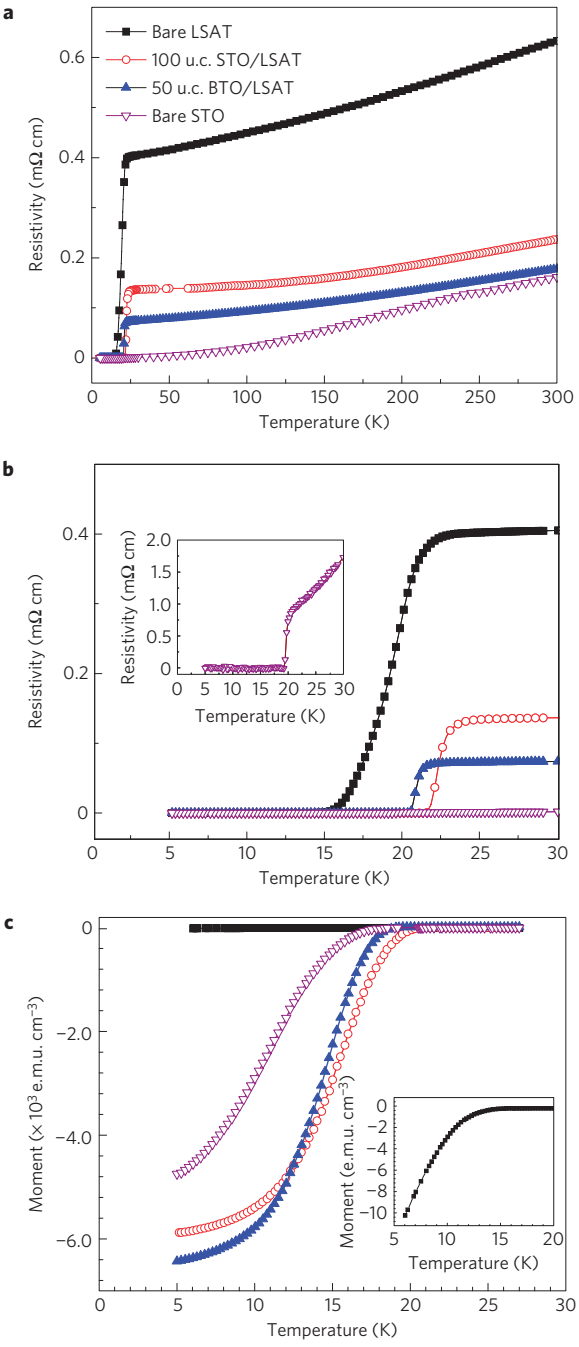

Figure 4 | Resistivity and magnetic moment as a function of temperature. **a**, $\rho(T)$ from room temperature to below T_c. **b**, Superconducting transition of all films; $T_{c,onset}$ and $T_{c,\rho=0}$ of the film on 100 u.c. STO/LSAT are as high as 22.8 K and 21.5 K, respectively. Inset: Superconducting transition of the film on bare STO. **c**, Magnetic moment as a function of temperature evaluated by warming after zero-field-cooling. A field of 2 mT was applied perpendicular to the plane of the films after cooling to 4.2 K. Inset: An expanded view of the much smaller diamagnetic signal of the film grown on bare LSAT.

We believe that two factors contribute to the high J_c. First, the films on templated LSAT and bare STO have high epitaxial quality with no high-angle tilt grain boundaries, as confirmed by both XRD and TEM analysis. According to our previous report[17], [001] tilt grain boundaries of Ba-122 with $\theta = 6°–24°$ show significant suppression of supercurrent, making it entirely understandable that randomly oriented high-angle tilt grain boundaries would effectively block supercurrent, as suggested by several recent pnictide film reports[10–12,14]. Indeed, the films grown on bare LSAT developed many high-angle grain boundaries, had almost no flux shielding even in low fields (2 mT) and very low J_c. In contrast, films on templated LSAT and bare STO showed high J_c without evidence of weak links. Interestingly, the J_c of the film on STO/LSAT is higher than that of the film on bare STO, which is consistent with our observation of a higher density of line defects in Ba-122 on STO/LSAT than for the film grown on bare STO. We also measured the angular-dependent transport J_c of a STO/LSAT film, as shown in Fig. 5b. J_c always shows a strong *c*-axis peak, which opposes the expected electronic anisotropy because the upper critical field H_{c2} is lower for H parallel to the *c* axis[23–25], making it clear that there is strong pinning along the Ba-122 *c* axis that is parallel to the vertically aligned defects of the secondary phases. Recently, a similar angular dependence was reported in much lower J_c but granular

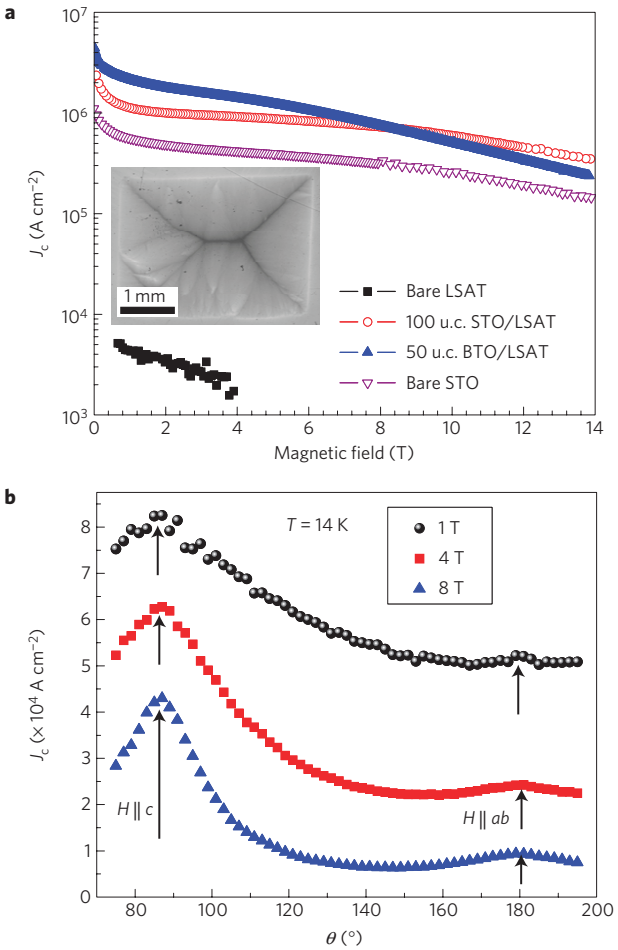

Figure 5 | J_c as a function of magnetic field and its angular dependence. **a**, Magnetization J_c as a function of magnetic field at 4.2 K with the field applied perpendicular to the plane of the film. Inset: A magneto-optical image obtained by zero-field-cooling to 6.6 K, then applying a magnetic 20 mT field perpendicular to the plane of the film. **b**, Transport J_c at 14 K and 1, 4 and 8 T as a function of the angle between the applied field and the surface of the Ba-122 films. The magnetic field is always perpendicular to the current-flow direction.

Co-doped Sr-122 films, which was associated with contributions from dilute magnetic pinning[26].

We have also grown Co-doped Ba-122 films on other bare substrates, including (001) LAO and (110) $GdScO_3$ (GSO). In spite of the almost perfect lattice match between Ba-122 and (110)-oriented GSO, the film on bare GSO shows poor quality, just like the films grown on bare LAO (see Supplementary Table SI). Both bare GSO and LAO films show broad peaks from misoriented grains in the ϕ scan. However, when an intermediate layer of STO or BTO was used as a template on the LAO or GSO, the properties of the Ba-122 films were markedly enhanced and misoriented grains were not seen. Remarkably, we could also grow a superior quality Ba-122 film on STO/GSO using template engineering with intermediate STO layers that produced a perfect lattice match with Ba-122. The FWHM of the (004) reflection rocking curve and $\Delta\phi$ of Ba-122 on 50 u.c. STO/GSO were very narrow, 0.24° and 0.3°, respectively (see Supplementary Table SI), values close to those of bulk single crystals[21]. All of the above results show that an STO or BTO template is the key to growing high-quality epitaxial Ba-122 films.

We have developed a versatile new method to turn granular, low-J_c superconducting films into single-crystal, high-J_c and truly epitaxial films of Ba-122. Our working hypothesis is that we are favouring bonding between the Ba alkaline-earth component of the pnictide phase and the underlying oxide substrate by using template engineering with the intermediate STO or BTO layers. Indeed, the J_c in our high-quality epitaxial films is about 10 times greater than in bulk single crystals[15] and ~400 times greater than in previously reported AE-122 films[10–12]. Template engineering permits truly single-crystal quality (Supplementary Table S1) without any loss of connectivity because of high-angle grain boundaries, and a high density of vertically aligned, secondary phase line defects results in strong *c*-axis pinning. We believe that this template technique can be applied not only to perovskite single-crystal substrates, but also to other types of oxide substrate or even semiconductor substrate. Indeed, we have demonstrated that this approach yields high-quality Co-doped Ba-122 films on an epitaxial STO template grown on (001) Si substrates[27,28] with $T_{c,\rho=0} = 18$ K, $\Delta T_c = 1$ K and no misoriented grains (see Supplementary Information). This approach thus greatly expands substrate choices for high-quality Ba-122 thin films, thus enabling much broader fundamental property investigations of the newly discovered ferropnictide superconductors and parent compounds, as well as exploration of their applications. Furthermore, we expect that epitaxial thin films of other layered intermetallics could be successfully grown on various types of oxide substrate by using similar template-engineering principles.

Methods

Co-doped Ba-122 thin films were grown *in situ* on various single-crystal substrates and STO- or BTO-templated substrates using pulsed laser deposition with a KrF (248 nm) ultraviolet excimer laser in a vacuum of 3×10^{-4} Pa at 730–750 °C. The base pressure before deposition was 3×10^{-5} Pa, and the deposition took place at 3×10^{-4} Pa because of degassing of the substrate heater. The Co-doped Ba-122 target was prepared by solid-state reaction with a nominal composition of Ba/Fe/Co/As = 1:1.84:0.16:2.2. The magnetization of the films that were about 2 mm × 4 mm was measured in a 14 T Oxford vibrating-sample magnetometer at 4.2 K with the applied field perpendicular to the film surface. Magneto-optical imaging was used to examine the uniformity of current flow in the films so as to validate the use of the Bean model for converting the magnetic moment measured in the vibrating sample magnetometer to J_c assuming current circulation across the whole sample without granular effects. For a thin film, $J_c = 15\,\Delta m/(Vr)$, where Δm is the width of the hysteresis loop in e.m.u., V is the film volume in cubic centimetres and r is the radius corresponding to the total area of the sample size, and was calculated from $\pi r^2 = a \times b$ (a and b are the film width and length in centimetres, respectively).

Received 28 September 2009; accepted 5 February 2010; published online 28 February 2010

References

1. Chaudhari, P., Koch, R. H., Laibowitz, R. B., McGuire, T. R. & Gambino, R. J. Critical-current measurements in epitaxial films of $YBa_2Cu_3O_{7-x}$. *Phys. Rev. Lett.* **58,** 2684–2686 (1987).
2. Oh, B. *et al.* Critical current densities and transport in superconducting $YBa_2Cu_3O_{7-\delta}$ films made by electron beam coevaporation. *Appl. Phys. Lett.* **51,** 852–854 (1987).
3. Eckstein, J. N. *et al.* Atomically layered heteroepitaxial growth of single-crystal films of superconducting $Bi_2Sr_2Ca_2Cu_3O_x$. *Appl. Phys. Lett.* **57,** 931–933 (1990).
4. Zeng, X. *et al. In situ* epitaxial MgB_2 thin films for superconducting electronics. *Nature Mater.* **1,** 35–38 (2002).
5. Bu, S. D. *et al.* Synthesis and properties of *c*-axis oriented epitaxial MgB_2 thin films. *Appl. Phys. Lett.* **81,** 1851–1853 (2002).
6. Kamihara, Y., Watanabe, T., Hirano, M. & Hosono, H. Iron-based layered superconductor $La[O_{1-x}F_x]FeAs$ ($x = 0.05$–0.12) with $T_C = 26$ K. *J. Am. Chem. Soc.* **130,** 3296–3297 (2008).
7. Chen, X.-H. *et al.* Superconductivity at 43 K in $SmFeAsO_{1-x}F_x$. *Nature* **453,** 761–762 (2008).
8. Wang, C. *et al.* Thorium-doping-induced superconductivity up to 56 K in $Gd_{1-x}Th_xFeAsO$. *Europhys. Lett.* **83,** 67006 (2008).
9. Rotter, M., Tegel, M. & Johrendt, D. Superconductivity at 38 K in the iron arsenide $Ba_{1-x}K_xFe_2As_2$. *Phys. Rev. Lett.* **101,** 107006 (2008).
10. Hiramatsu, H., Katase, T., Kamiya, T., Hirano, M. & Hosono, H. Superconductivity in epitaxial films of Co-doped $SrFe_2As_2$ with bilayered FeAs structures and their magnetic anisotropy. *Appl. Phys. Express* **1,** 101702 (2008).

11. Katase, T. *et al.* Atomically-flat, chemically-stable, superconducting epitaxial thin film of iron-based superconductor, cobalt-doped $BaFe_2As_2$. *Solid State Commun.* **149,** 2121–2124 (2009).
12. Choi, E. M. *et al. In situ* fabrication of cobalt-doped $SrFe_2As_2$ thin films by using pulsed laser deposition with excimer laser. *Appl. Phys. Lett.* **95,** 062507 (2009).
13. Hiramatsu, H., Katase, T., Kamiya, T., Hirano, M. & Hosono, H. Heteroepitaxial growth and optoelectronic properties of layered iron oxyarsenide, LaFeAsO. *Appl. Phys. Lett.* **93,** 162504 (2008).
14. Haindl, S. *et al.* $LaFeAsO_{1-x}F_x$ thin films: High upper critical fields and evidence of weak link behaviour. Preprint at <http://arxiv.org/abs/0907.2271v1> (2009).
15. Yamamoto, A. *et al.* Small anisotropy, weak thermal fluctuations, and high field superconductivity in Co-doped iron pnictide $Ba(Fe_{1-x}Co_x)_2As_2$. *Appl. Phys. Lett.* **94,** 062511–062513 (2009).
16. Kametani, F. *et al.* Intergrain current flow in a randomly oriented polycrystalline $SmFeAsO_{0.85}$ oxypnictide. *Appl. Phys. Lett.* **95,** 142502 (2009).
17. Lee, S. *et al.* Weak link behaviour of grain boundaries in superconducting $Ba(Fe_{1-x}Co_x)_2As_2$ bicrystals. *Appl. Phys. Lett.* **95,** 212505 (2009).
18. Herranz, G. *et al.* High mobility in $LaAlO_3/SrTiO_3$ heterostructures: Origin, dimensionality, and perspectives. *Phys. Rev. Lett.* **98,** 216803 (2007).
19. Zhang, X. *et al.* Josephson effect between electron-doped and hole-doped iron pnictide single crystals. *Appl. Phys. Lett.* **95,** 062510 (2009).
20. Rijnders, G. J. H. M. *et al. In situ* monitoring during pulsed laser deposition of complex oxides using reflection high energy electron diffraction under high oxygen pressure. *Appl. Phys. Lett.* **70,** 1888–1890 (1997).
21. Wang, X. F. *et al.* Anisotropy in the electrical resistivity and susceptibility of superconducting $BaFe_2As_2$ single crystals. *Phys. Rev. Lett.* **102,** 117005 (2009).
22. Sefat, A. S. *et al.* Superconductivity at 22 K in Co-doped $BaFe_2As_2$ crystals. *Phys. Rev. Lett.* **101,** 117004 (2008).
23. Yamamoto, A. *et al.* Small anisotropy, weak thermal fluctuations, and high field superconductivity in Co-doped iron pnictide $Ba(Fe_{1-x}Co_x)_2As_2$. *Appl. Phys. Lett.* **94,** 062511 (2009).
24. Yuan, H. Q. *et al.* Nearly isotropic superconductivity in $(Ba,K)Fe_2As_2$. *Nature* **457,** 565–568 (2009).
25. Baily, S. A. *et al.* Pseudoisotropic upper critical field in cobalt-doped $SrFe_2As_2$ epitaxial films. *Phys. Rev. Lett.* **102,** 117004 (2009).
26. Maiorov, B. *et al.* Angular and field properties of the critical current and melting line of Co-doped $SrFe_2As_2$ epitaxial films. *Supercond. Sci. Technol.* **22,** 125011 (2009).
27. McKee, R. A., Walker, F. J. & Chisholm, M. F. Crystalline oxides on silicon: The first five monolayers. *Phys. Rev. Lett.* **81,** 3014–3017 (1998).
28. Goncharova, L. V. *et al.* Interface structure and thermal stability of epitaxial $SrTiO_3$ thin films on Si(001). *J. Appl. Phys.* **100,** 014912 (2006).

Acknowledgements

We are grateful to J. Fournelle, M. Putti, A. Xu, F. Kametani, A. Gurevich, P. Li and V. Griffin for discussions and experimental help. Work at the University of Wisconsin was supported by funding from the DOE Office of Basic Energy Sciences under award number DE-FG02-06ER46327, and that at the NHMFL was supported under NSF Cooperative Agreement DMR-0084173, by the State of Florida and by AFOSR under grant FA9550-06-1-0474. A.Y. is supported by a fellowship of the Japan Society for the Promotion of Science. All TEM work was carried out at the University of Michigan and was supported by the Department of Energy under grant DE-FG02-07ER46416.

Author contributions

S.L. fabricated Ba-122 thin-film samples and prepared the manuscript. J.J. carried out electromagnetic characterization and prepared the manuscript. J.D.W. fabricated Ba-122 pulsed laser deposition targets for thin-film deposition. C.W.B., H.W.J., C.M.F. and J.W.P. fabricated thin-film templates on single-crystal substrates. C.T., A.P., D.A. and A.Y. carried out electromagnetic characterizations. S.H.B. and C.W.B. analysed epitaxial arrangement by X-ray diffraction. Y.Z. and C.T.N. carried out TEM measurements. C.B.E., D.C.L., E.E.H. and X.Q.P. supervised the experiments and contributed to manuscript preparation. C.B.E. designed and directed the research. All authors discussed the results and implications and commented on the manuscript at all stages.

Additional information

The authors declare no competing financial interests. Supplementary information accompanies this paper on www.nature.com/naturematerials. Reprints and permissions information is available online at http://npg.nature.com/reprintsandpermissions. Correspondence and requests for materials should be addressed to C.B.E.